Armenian Journal of Physics, 2019, vol. 12, issue 3, pp. 261-272

Magnetic Properties and Entanglement of Nickel Containing Polymer

(Proceedings of the Int. Conference on "The Problems of Modern Condensed Matter Physics")

V. Abgaryan[1], N. Ananikian[2,3], L. Ananikyan[2], H. Poghosyan[2]

[1] *Laboratory of Information Technologies, Joint Institute for Nuclear Research, 6 Joliot-Curie St, 141980 Dubna, Russia*
[2] *Alikhanyan National Science Laboratory, Alikhanian Br. 2, 0036 Yerevan, Armenia*
[3]*CANDLE Synchrotron Research Institute, Acharyan 31, 0040 Yerevan, Armenia*
E-mail: ananik@yerphi.am

Received: 30 June 2019

Abstract. We establish an exactly solvable Heisenberg-Ising modification of spin-1 Ni-containing polymer chain model, for [*Ni(NN'-dmen)(μ-N$_3$)$_2$*], with *NN'-dmen* being *NN'-dimethlethyledediamine*. The material has been partly studied in experiment but not for its behavior of magnetization plateaus and magnetic susceptibility at low temperatures. By exact solution, we show that the magnetization exhibits three plateaus at zero, mid, and 3/4 of the saturation value at low temperatures, when interaction parameters lie in the vicinity of the values recovered by fitting through fully Heisenberg model. The corresponding featuring peaks of magnetic susceptibility are clearly shown. We have also calculated the susceptibility in zero magnetic field versus the temperature which shows a peak around *T = 12.6 K*, which is compatible with the experimental results. The model also displays plateaus in thermal entanglement that capture the one-to-one correspondence between thermal entanglement and magnetization.

Keywords: quantum spin model, metal-containing polymer, magnetization plateaus, susceptibility peaks

1. Introduction

The μ-azido bridging ligand with divalent metal ions, mainly Cu^{II}, Ni^{II}, Co^{II}, Cd^{II}, Fe^{II}, and Mn^{II} [1, 2] is a very good candidate and one of the most adaptable and flexible ones for creating new materials with different magnetic properties. Besides, it is very functional in the studying of magnetization structure and magnetic correlations both in discrete and polymeric complexes. The nitrogen μ-azido may give end-to-end (EE) or end-on (EO) coordination modes, where normally, the first ones cause antiferromagnetic couplings and the latter ones result in ferromagnetic couplings [3]. Much work has been devoted to the control and design of high spin metal-azide [4] systems by incorporating different organic ligands, transition metal coordination polymers with azide and flexible zwitterionic dicarboxylate ligands [5, 6] polynuclear Mn(II)-azido bridging compounds have been experimentally measured and synthesized by [7]. Therefore, it would be potentially interesting to study the appearance of these coordination modes with relation to probable occurring magnetization plateaus in these systems, especially for long polymer chains. Magnetization plateau is observed in spin-half tetramer chain of copper compound $Cu(3-Clpy)_2(N_3)_2$ ($3-Clpy = 3-$chloropyridine, C_5H_4NCl), with ferromagnetic-ferromagnetic-antiferrmagnetic-antiferromagnetic bond alternating interactions [8-10].

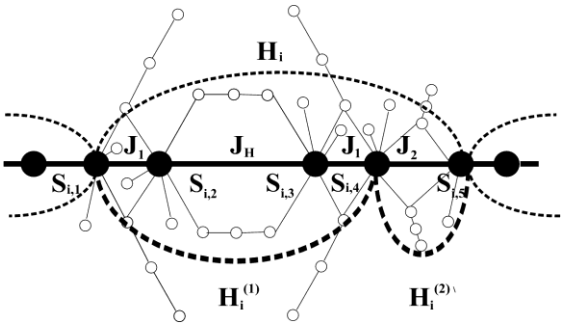

Figure 1. The schematic representation of the chain with the underlying molecular structure of spin-1 Ni -containing polymer $[Ni(NN'-dmen)(\mu-N_3)_2]$. The filled circles represent Ni atoms, the smaller empty circles N atoms; the bonds between the atoms are represented by light lines while the effective magnetic couplings by solid lines (the representation is purely schematic and the relative bond lengths and angles may deviate from true values. See [3] for more details on the molecular structure).

Ribas et. al. in their experimental work [3] reported that they synthesized and fully characterized a new Ni^{II} -compound, with chemical formula, $[Ni(NN'-dmen)(\mu-N_3)_2]$, where $NN'-dmen$ is $NN'-$ dimethylethylenediamine that exhibits the two kinds of coordination mode at the same time (Figure 1). The molecular structure consists of Ni^{II} ions centers alternatively linked by three double EO entities and one double EE entity. Each Ni^{II} ion completes its distorted octahedral coordination by binding to one bidentate $NN'-dmen$ ligand. Their theoretical results were obtained by considering a short Heisenberg quantum system with two blocks and periodic boundary conditions. Ribas et. al. in their calculations did not obtain the maximum magnetic susceptibility. We calculated the magnetic susceptibility at zero external magnetic field for the same two Heisenberg blocks of quantum system consisting of 8 nickel atoms with periodic boundary condition including the peak at low temperature ($T \approx 12$). The exact solution of the model was obtained by parallel computing (Wolfram Mathematica Language) in two pure Heisenberg blocks. The best fit to the experimental data presented by Ribas et. al. was obtained by introducing a anisotropy parameter δ in the following way: $\vec{S_i}\vec{S_j} = \delta(S_i^x S_j^x + S_i^y S_j^y) + S_i^z S_j^z$ where i and j are adjacent spins corresponding to coupling constants J_1 or J_2. The susceptibility and susceptibility times temperature for $\delta = 1.44$ is shown in Figure 2.

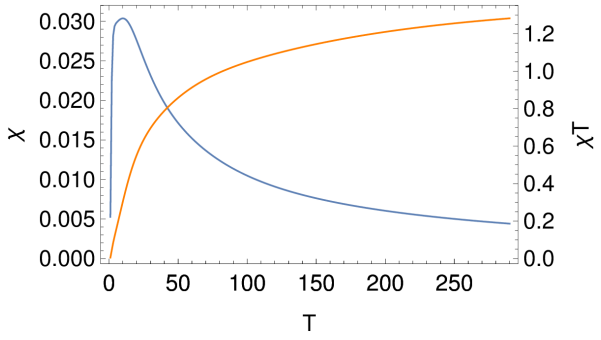

Figure 2. Magnetic susceptibility at zero external magnetic field for the two Heisenberg blocks quantum system with anisotropy parameter consisting of 8 nickel atoms with periodic boundary condition. The blue graph is and orange one.

Here we report on the magnetic properties of the same polymer through introducing an exactly solvable model that truly describes the interaction characteristics of the spin-1 Ni-containing polymer [3] at low temperatures. There are some differences in the susceptibility for a long Ising-Heisenberg model and eight spin quantum Heisenberg model. Moreover the best fit to the short systems experimental data was obtained by introducing the anisotropy parameter. Nevertheless the magnetization curves for the same parameters of the long Ising-Heisenberg and short quantum Heisenberg models are very similar (see Figure 3). Thermal entanglement, quantum correlations and magnetization plateaus of Spin 1 and $1/2$ Isning-Heisenberg models on diamond chains have been carefully studied [11-15]. We also look into negativity as a measure to observe quantum correlations and entanglement of the polymer. In section 2, we introduce the model Hamiltonian with a block composition and provide its exact solution. In section 3, we discuss the ground state and its phase diagram.

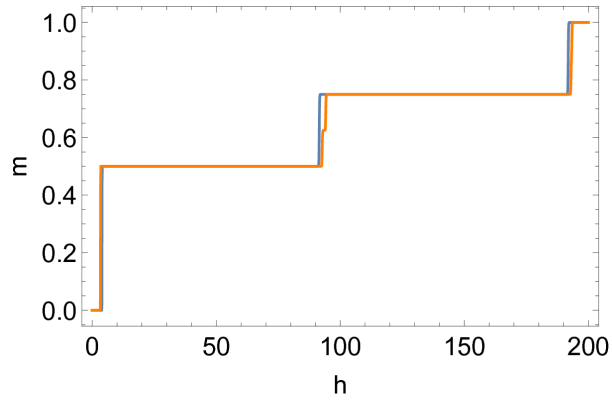

Figure 3. Magnetization (m) of the quantum eight Heisenberg spins (orange) and Ising-Heisenberg (blue) models for the standard configuration depending on the external magnetic field (h).

In section 4, we see the appearance of the magnetization plateaus and the susceptibility peaks and in section 5 we show the corresponding behavior of the quantum entanglement of the model. Finally, we give the conclusions.

2. Solvable spin-1 model Hamiltonian

The Ising-Heisenberg chain Hamiltonian has the form $H=\sum_{i=1}^{N}(H_i^{(1)}+H_i^{(2)})$ with

$$H_i^{(1)}=-J_H\vec{S}_{i,2}.\vec{S}_{i,3}-J_1\left(S_{i,1}^zS_{i,2}^z+S_{i,3}^zS_{i,4}^z\right)-g\mu_Bh\left(\frac{1}{2}S_{i,1}^z+S_{i,2}^z+S_{i,3}^z+\frac{1}{2}S_{i,4}^z\right)$$

$$+D\left(\frac{1}{2}(S_{i,1}^z)^2+(S_{i,2}^z)^2+(S_{i,3}^z)^2+\frac{1}{2}(S_{i,4}^z)^2\right), \qquad (1)$$

$$H_i^{(2)}=-J_2S_{i,4}^zS_{i,5}^z-\frac{1}{2}\left(g\mu_Bh\left(S_{i,4}^z+S_{i,5}^z\right)+D\left(\left(S_{i,4}^z\right)^2+\left(S_{i,5}^z\right)^2\right)\right),$$

captures the interaction structure in the polymer $[Ni(NN'-dmen)(\mu-N_3)_2]$,

(Figure 1). In equation (1), $\vec{S}_{i,k}$ is the vector operator of spin-1 at site k of the i-th block and $S^z_{i,k}$ is its corresponding z-component. Cyclic boundary conditions are applied in the thermodynamic limit. The parameters J_1 and J_2 are bilinear Ising ferromagnetic coupling constants, J_H is Heisenberg antiferromagnetic exchange coupling, and D is single-ion anisotropy, while the external magnetic field is given by h, whereas g and μ_B are the Land\'{e} factor and the Bohr magneton respectively.

After the exact solution of the model, when we construct magnetization and susceptibility, as long as it does not affect the qualitative nature of the results, we take the coupling constants and the anisotropy in the vicinity of values obtained in [1-3], namely $J_1 = 20cm^{-1}$, $J_2 = 37cm^{-1}$, $J_H = -120cm^{-1}$, and $D = -6cm^{-1}$, $g = 2.39$.

Our exact calculations, based on the Hamiltonian H with small bilinear Ising ferromagnetic and rather large Heisenberg antiferromagnetic couplings completely matches experimental results reported in the literature [3].

2.1. The transfer-matrix approach

We observe that the model of the polymer is actually composed of N separable blocks each of which consists of 5 spins. Notice that the first and fifth spins of each block are shared by the neighboring blocks (Figure 1). The commutator of $[H, H_i]$ is equal to zero $H_i = H_i^{(1)} + H_i^{(2)}$ and therefore the standard expression for the partition function $Z = tr\left(e^{-\beta H}\right)$ may represented as

$$Z = tr\prod_{i=1}^{N} e^{-\beta H_i},$$

where $\beta = \frac{1}{k_B T}$, with temperature T temperature and Boltzmann constant $k_B \approx 0.695\, cm^{-1}K^{-1}$. Furthermore, utilizing the Ising (diagonal) nature of interaction between neighboring blocks, under the trace operation we assume that operators $S^z_{i,1}$ and $S^z_{i,5}$ are replaced with mere numbers $s_{i,1}$ and $s_{i,5}$ which independently take values $-1,0,1$ (because they are classical Ising spins).

In this notation the partition function transforms into

$$Z = \sum_{\{s_{i,1},s_{i,5}=-1,0,1|i=1\ldots N\}} \prod_{i=1}^{N} tr\left(e^{-\beta H_i(s_{i,1},s_{i,5})}\right) = tr(W^N). \quad (2)$$

Here, the transfer matrix is $W = \| W \|_{s_1,s_5} = tr\left(e^{-\beta H_i(s_1,s_5)}\right)$.

Instead of considering a single transfer-matrix we could consider a double-block computation approach with generating sub-Hamiltonians $H_i^{(1)}$ and $H_i^{(2)}$ in which we have a block of four spins followed by a block of two spins, where the first and last spins of each block are always shared with the neighboring blocks (see Figure 1.) and $W = W^{(1)}W^{(2)}$. The two approaches would obviously give the same results. In our calculations, on the basis of transfer matrix for the blocks, we would face a not very common case in which the transfer matrices of the two sub-blocks are symmetric while the product of them which gives the transfer matrix of the whole block of 5 particles is non-symmetric positive (see [16], for example.). As it is well known, W would be similar to a matrix in Jordan canonical form. Hence $trW = trJ$, where J is the Jordan form of W. Given that the transfer matrix is a matrix of positive elements, according to Perron-Frobenius theorem, we know that the eigenvalue with the largest absolute value would be real (An alternative approach would be a representation of the partition function as $Z = tr(\tilde{W}^N)$, where $\tilde{W} = \sqrt{W^{(1)}}W^{(2)}\sqrt{W^{(1)}}$ is a symmetric (hence diagonalizable) real matrix.).

Now, the free energy and magnetization per site (in units of saturation value) in thermodynamic limit are respectively given as $f = -\frac{1}{4N\beta}\ln Z = -\frac{1}{4\beta}\ln\lambda_{Max}$ and $m = -\frac{1}{g\mu_B}\frac{\partial F}{\partial h}$.

2.2. Diagonalizing the block Hamiltonian

In order to obtain the explicit form of the partition function one needs the exact form of the transfer matrix and hence the diagonal form of the block Hamiltonian. To diagonalize the Hamiltonian H_i we remember that $[H, S_i^z] = [H_i, S_i^z] = [H_i, \sum_{j,1}^{4} S_{i,j}^z] = 0$, which implies the existence of a common eigenbasis for H_i and S_i^z. By performing a unitary transformation to a representation where the eigenvectors of S_i^z are sorted by decreasing order of corresponding eigenvalues we bring the 243×243 Hamiltonian H_i to a block diagonal form. Further the commutation relations $[H_i, S_{i,j}^z] = 0$ ($j = 1,4,5$) help us to make ordering inside the blocks by the same rule bringing H_i to the maximally arranged block diagonal form $\tilde{H}$

$$\tilde{H} = \bigoplus_{s_1,s_4,s_5=-1,0,1} \left(\mathfrak{A}^{+}(s_1,s_4,s_5)\oplus\mathfrak{A}^{-}(s_1,s_4,s_5)\oplus\mathfrak{B}^{+}(s_1,s_4,s_5)\oplus\mathfrak{B}^{-}(s_1,s_4,s_5)\oplus\mathfrak{C}(s_1,s_4,s_5)\right),$$

$$\left[H_i\right]_{243\times243} = diagonal\Big[\Big\{\left[\mathfrak{A}^{+}\left(s_1,s_4,s_5\right)\right]_{1\times1},\left[\mathfrak{A}^{-}(s_1,s_4,s_5)\right]_{1\times1},\left[\mathfrak{B}^{+}(s_1,s_4,s_5)\right]_{2\times2},$$

$$\left[\mathfrak{B}^{-}(s_1,s_4,s_5)\right]_{2\times2},\left[\mathfrak{C}(s_1,s_4,s_5)\right]_{3\times3}\Big\}\Big|\, s_1,s_4,s_5 == -1,0,1\Big],$$

$$\mathfrak{A}^{\pm} = d(s_1,\pm1,\pm1,s_4,s_{i,5}),\quad \mathfrak{B}^{\pm} = \begin{pmatrix} d(s_1,\pm1,0,s_4,s_5) & -J_H \\ -J_H & d(s_1,0,\pm1,s_4,s_5)\end{pmatrix}, \tag{3}$$

$$\mathfrak{C} = \begin{pmatrix} d\left(s_1,1,-1,s_4,s_5\right) & -J_H & 0 \\ -J_H & d\left(s_1,0,0,s_4,s_5\right) & -J_H \\ 0 & -J_H & d\left(s_1,-1,1,s_4,s_5\right)\end{pmatrix}, \tag{4}$$

and

$$d(s_1,s_2,s_3,s_4,s_5) = \frac{1}{2}\Big(D\left(s_1^2+s_5^2+2\left(s_2^2+s_3^2+s_4^2\right)\right)-\mu_B g h\left(s_1+2\left(s_2+s_3+s_4\right)+s_5\right)$$

$$-2\left(s_3s_2J_H+J_1\left(s_1s_2+s_3s_4\right)+J_2s_4s_5\right)\Big). \tag{5}$$

Is the fully Ising analogue of the block Hamiltonian. Thus, it is clear that $\mathfrak{A}^{\pm}(s_1,s_2,s_3,s_4,s_5)$'s are themselves eigenvalues of H_i. All left to do is to diagonalize $\mathfrak{B}^{\pm}$ and $\mathfrak{C}$ to arrive to the following final expressions for the eigenvalues of H_i.

$$E^{\mathfrak{A}^{\pm}}(s_1,s_4,s_5) = \mathfrak{A}^{\pm}(s_1,s_4,s_5),$$

$$E^{\mathfrak{B}^{\pm}}_{1,2}(s_1,s_4,s_5) = \frac{1}{2}\Big(d\left(s_1,\pm1,0,s_4,s_5\right)+d\left(s_1,0,\pm1,s_4,s_5\right)\pm\sqrt{\left(d\left(s_1,\pm1,0,s_4,s_5\right)-d\left(s_1,0,\pm1,s_4,s_5\right)\right)^2+4J_H^2}\Big), \tag{6}$$

$$E^{\mathfrak{C}}_1(s_1,s_4,s_5) = -\frac{1}{3}c_2+(C+T),\quad E^{\mathfrak{C}}_{2,3}(s_1,s_4,s_5) = -\frac{1}{3}c_2-\frac{1}{2}(C+T)\pm\frac{1}{2}i\sqrt{3}(C-T)$$

with the following notations

$$C = \sqrt[3]{R+\sqrt{F}},\quad T = \sqrt[3]{R-\sqrt{F}},\quad F = Q^3+R^2,\quad Q = \frac{3c_1-c_2^2}{9},$$

$$R = \frac{9c_2c_1-27c_0-2c_2^3}{54}, c_0 = -\frac{1}{6}\left(t_1^3-3t_2t_1+2t_3\right), \tag{7}$$

$$c_1 = \frac{1}{2}\left(t_1^2 - t_2\right), \quad c_2 = -t_1, \quad t_k = Tr(\mathfrak{C}^k).$$

Now, the transfer matrix is representable as

$$W(s_1, s_5) = \sum_{s_4, \alpha = \mathfrak{A}^{\pm}, \mathfrak{B}^{\pm}, \mathfrak{C}} e^{-\beta E^{\alpha}(s_1, s_4, s_5)} \tag{8}$$

3. Ground state of the polymer

Let us now briefly describe the ground state phases of the spin-1 $[Ni(NN' - dmen)(\mu - N_3)_2]$ in the vicinity of the values of parameters described in [3]. Figure (4) shows the phase diagram for different values of the antiferromagnetic Heisenberg coupling constant J_H and magnetic field h. There are four distinguished phases in the phase diagram, one Saturated Paramagnetic Phase (SPA) and three Quantum Antiferromagnetic Phases (QAF).

$$|SPA\rangle = \bigotimes_{i=1}^{N} |1,1,1,1\rangle_i \quad m = 1, \qquad |QAF1\rangle = \bigotimes_{i=1}^{N} \frac{1}{\sqrt{2}}(|1,0,1,1\rangle - |1,1,0,1\rangle)_i \qquad m = \frac{3}{4},$$

$$|QAF2\rangle = \bigotimes_{i=1}^{N} |1\rangle_i \otimes \Big[\frac{2|J_H|}{\sqrt{8J_H^2 + \left(2D + J_H + \lambda\right)^2}}\left(|1,-1\rangle + \frac{\left(2D + J_H + \lambda\right)}{2J_H}|0,0\rangle + |-1,1\rangle\right)\Big]_i \otimes |1\rangle_i$$

where $m = \frac{1}{2}$, (9)

$$|QAF3\rangle = \bigotimes_{i=1}^{N} |\pm(-1)^i\rangle_i \otimes \Big[\frac{1}{\sqrt{1 + a^2 + \left(1 - ab\right)^2}}\left(|-1,1\rangle - \left(1 - ab\right) \times |0,0\rangle + a|1,-1\rangle\right)\Big]_i \otimes |\pm(-1)^{i+1}\rangle_i,$$

where $m = 0$,

$$\begin{aligned} \lambda &= \sqrt{(2D + J_H)^2 + 8J_H^2}, \\ a &= \alpha_i(\pm(-1)^i, 0, 0, \pm(-1)^{i+1}, \pm(-1)^{i+1}) \\ b &= \alpha_i(\pm(-1)^i, -1, 1, \pm(-1)^{i+1}, \pm(-1)^{i+1}), \end{aligned} \tag{10}$$

and

$$\alpha(s_{i,1}, s_{i,2}, s_{i,3}, s_{i,4}, s_{i,5}) = \frac{1}{J_H}\left(d(s_{i,1}, s_{i,2}, s_{i,3}, s_{i,4}, s_{i,5}) - E_i(s_{i,1}, s_{i,4}, s_{i,5})\right),$$

$E_i(s_1, s_4, s_5)$ is the eigenvalue of H_i corresponding to the i-th block of $|QAF3\rangle$, such that $E_i = E_2^{\mathfrak{C}}(\pm(-1)^i, \pm(-1)^{i+1}, \pm(-1)^{i+1})$ (see eq. (4) and eq. (6).

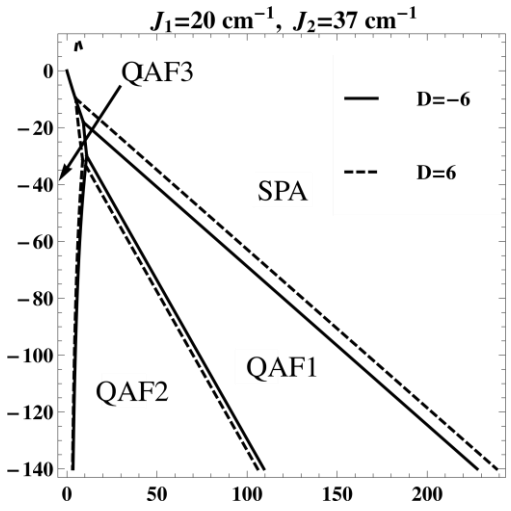

Figure 4. Ground State Phase Diagram of the spin-1 $[Ni(NN'-dmen)(\mu-N_3)_2]$ polymer for different values of J_H and magnetic field h and for $J_1 = 20cm^{-1}$, $J_2 = 37cm^{-1}$, and $D = -6cm^{-1}$

4. Magnetic properties of the polymer

Our calculations show that at low temperatures, with magnetic field, three magnetization plateaus at 0, $\frac{1}{2}$, and $\frac{3}{4}$ of the saturation value are observable, which are clearly shown in Fig (5) versus the applied magnetic field h and the temperature T. Fig (5) also shows the first plateau along with part of the second one for values of 0 to 6 *Tesla* of the applied magnetic field and in temperatures below $2K$.

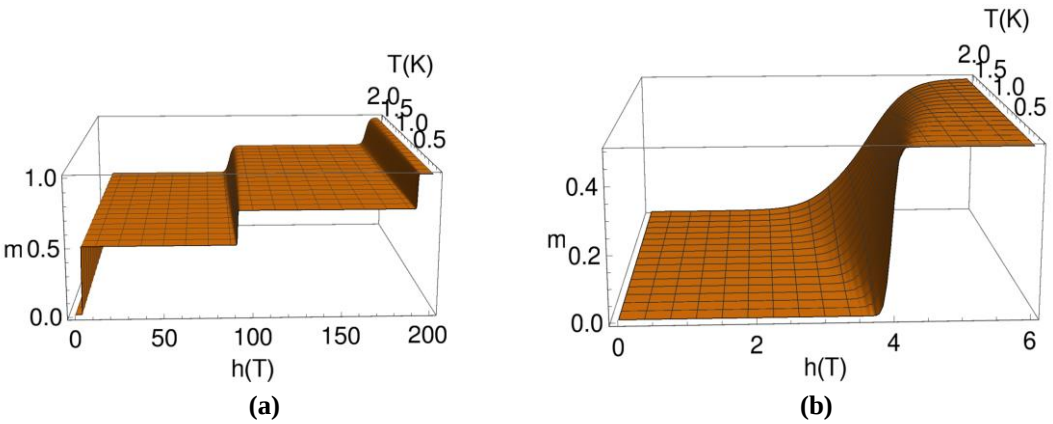

Figure 5. (a) magnetization behavior of the spin-1 $[Ni(NN'-dmen)(\mu-N_3)_2]$ polymer as a function of the absolute temperature T in *Kelvin* and the magnetic field h in *Tesla*. (b): the zero- and 1/2-plateau of the magnetization is showing. Magnetization has no units.

Magnetization plateaus occur both in antiferromagnetic and ferromagnetic materials and they play an essential role in understanding a large family of nontrivial quantum phenomena. The phenomenon of magnetization plateau is considered as a macroscopic manifestation of the essentially quantum effect in which the magnetization m is quantized at fractional values of the saturation magnetization m_s. The quantum plateau state was actually first discovered over two decades ago [17]. One of the first experimental observations was reported in a diamond chain [18]. Magnetization plateau has been studied during the past decade both experimentally and theoretically in spin-1 models [19-23].

We have considered an infinite chain and exactly calculated its magnetization plateaus as in ref. [15]. But we also regarded finite chains with all Heisenberg interactions versus Heisenberg-Ising interactions as in the Hamiltonian (1). We considered chains of one block ($N=1$) with four spins and two blocks ($N=2$) with eight spins with cyclic boundary conditions. The results for magnetization plateaus are almost the same for the mid-plateau and 3/4-plateau except that their horizontal positions on magnetic field h axis are slightly shifted with respect to each other, while zero-plateau would disappear.

In accordance with the appearance of three plateaus in the magnetization graph, we observe three corresponding peaks in the magnetic susceptibility as a function of the applied magnetic field h and the temperature T.

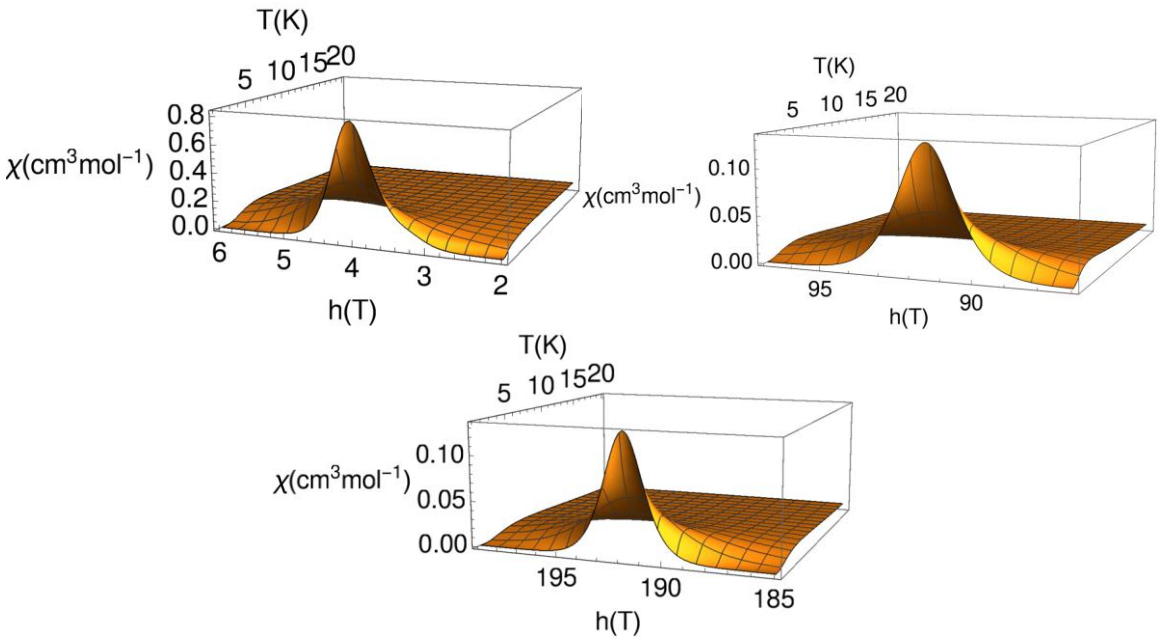

Figure 6. The three peaks of the magnetic susceptibility of the spin-1 $[Ni(NN'-dmen)(\mu-N_3)_2]$ polymer as a function of the absolute temperature $T(K)$ and the magnetic field $h(T)$ at low temperatures. Magnetic susceptibility χ is measured in cm^3mol^{-1}.

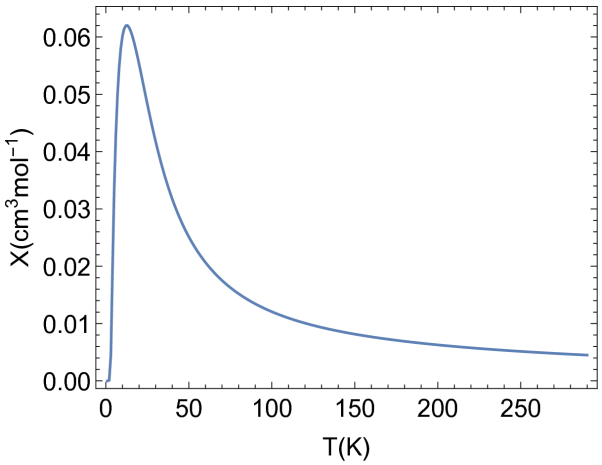

Figure 7. Plot of magnetic susceptibility χ versus the temperature in zero magnetic field for $[Ni(NN'-dmen)(\mu-N_3)_2]$ polymer

The magnetic susceptibility of a material is equal to the ratio of the magnetization m within the material to the applied magnetic field strength h. This ratio, strictly speaking, is the volume susceptibility, because magnetization essentially involves a certain measure of magnetism (dipole moment) per unit volume. For single Ni - containing polymer with cyclic boundary condition in the thermodynamic limit, the molar magnetization m is has the dimensions of cm^3Tmol^{-1} and the molar magnetic susceptibility χ has the dimension of cm^3mol^{-1}. The characteristic peaks of the magnetic susceptibility can be seen in the low temperatures see Figure 6.

We have also calculated the susceptibility in zero magnetic field versus the temperature which is shown in Figure 7 and has a peak around $T=12.6K$, which is compatible with the result from [3].

5. Thermal negativity of Ni -containing polymer

Entanglement is a type of correlation that is quantum mechanical in nature. Studying entanglement in condensed matter systems is of great interest due to the fact that some behaviors of such systems can most probably only be explained with the aid of entanglement. The magnetic susceptibility at low temperatures, quantum phase transitions, chemical reactions are examples where the entanglement and correlation functions are the key ingredients for a complete understanding of the system [24-28]. Furthermore, in order to produce a quantum processor, the entanglement in condensed matter systems becomes an essential concept. On the other hand, in systems like some molecular magnetic materials, the magnetic susceptibility can be directly related to an entanglement witness (EW) [29]. Thermal negativity and magnetization plateaus of spin-1 particles in a diamond chain Ising - Heisenberg model has been recently studied in [12, 20].

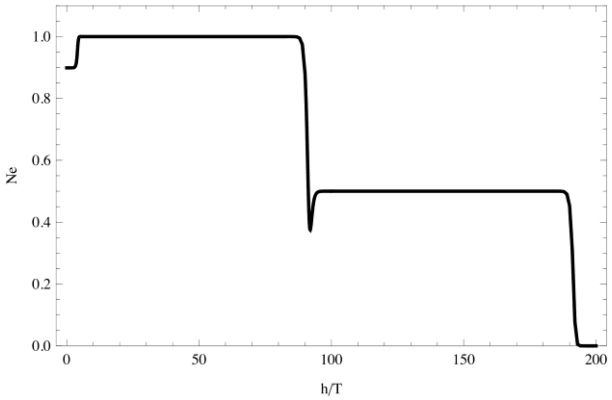

Figure 8. The plateaus of the negativity in correspondence with the magnetization plateaus

We calculated negativity as a calculable measure of thermal entanglement [30] in Ni-containing $[Ni(NN'-dmen)(\mu-N_3)_2]$ polymer of spin-1 particles with Heisenberg-Ising interactions. For that purpose, we used the reduced density matrix ρ of the pair of particles with Heisenberg interaction between them in the block. To find out the reduced density matrix ρ in the r the block, we need to trace out all the degrees of freedom except for the 2nd and 3rd spin in block r. To accomplish such a calculation, we followed a method similar to the one that is described in [20] through which, the reduced density matrix ρ is derived in terms of the transfer matrix. Then the amount of entanglement between the two particles would be given by $Ne=\frac{\| \rho^{T_A} \|_1 -1}{2}$, where ρ^{T_A} is the partial transpose of ρ with respect to any one of its subsystems meaning any one of the spins coupled with antiferroagnetic Heisenberg exchange, whose elements are $\langle \alpha\gamma | \rho^{T_A} | \beta\delta \rangle = \langle \beta\gamma | \rho | \alpha\delta \rangle$ and $\| X \|_1$ is the trace norm of X, which is $Tr\sqrt{X^{\dagger}X}$ by definition. The result is showing in Figure 8. We can see the one to one correspondence between the negativity plateaus and those of the magnetization in Figure 5.

6. Conclusion

We introduced and explored a compatible theory model of a Ni-containing polymer for a long chain that can fully cover and explain the experimental data which was gained and reported in [3] we also obtained the peak of magnetic susceptibility for the model described by Ribas. Along with studying magnetic properties of the model, we investigated quantum entanglement by calculating the negativity for the Heisenberg-interacting pair in the model and noticed a very good agreement with the magnetization at low temperatures. We conducted our calculations on the basis of the transfer matrix method for separable blocks, where each two consecutive blocks would have their first and last spins in common. This study would enhance our understanding of nitrogen μ-azido ligand as one of the most adaptable entities to be exploited to create new materials both discrete and polymeric while playing a key role in determining the relative magnetic properties of the materials. This is especially true for the low-temperature behavior of this ingredient since there is no experimental result for magnetic

plateaus and other magnetic properties of Ni-containing polymer, $[Ni(NN'-dmen)(\mu-N_3)_2]$ at low temperatures.

Acknowledgements

This work was supported by the CS MES RA in the frame of the Research Projects № 18T-1C155 and № 19YR-1C076 grants.

References

[1] Joan Ribas, Albert Escuer, Montserrat Monfort, Ramon Vicente, Roberto Cort´es, Luis Lezama, and Teofilo Rojo. Coordination Chemistry Reviews **193** (1999) 1027–1068.
[2] Franz A Mautner, Michael Scherzer, Christian Berger, Roland C Fischer, Ramon Vicente, and Salah S Massoud. Polyhedron **85** (2015) 329–336.
[3] Joan Ribas, Montserrat Monfort, Immaculada Resino, Xavier Solans, Pierre Rabu, Fabrice Maingot, and Marc Drillon. Angewandte Chemie International Edition in English **35** (1996) 2520– 2522.
[4] Xiao li Yu, Wan sheng You, Xin Guo, Lan cui Zhang, Yan Xu, Zhen gang Sun, and Rodolphe Cl´erac. Inorganic Chemistry Communications **10** (2007) 1335–1338.
[5] Yu Ma, Jian-Yong Zhang, Ai-Ling Cheng, Qian Sun, En-Qing Gao, and Cai-Ming Liu. Inorganic Chemistry **48** (2009) 6142–6151.
[6] S. Khani, M. Montazerozohori, A. Masoudiasl, and J.M. White. Journal of Molecular Structure, **1153** (2018) 239–247.
[7] Franz A. Mautner, Christian Berger, Michael Scherzer, Roland C. Fischer, Lindley Maxwell, Eliseo Ruiz, and Ramon Vicente. Dalton Transactions **44** (2015) 18632–18642.
[8] Masayuki Hagiwara, Yasuo Narumi, Kazuhiko Minami, Koichi Kindo, Hideaki Kitazawa, Hiroyuki Suzuki, Naoto Tsujii, and Hideki Abe. Journal of the Physical Society of Japan **72** (2003) 943–946.
[9] Jozef Strečka, Michal Jăsčur, Masayuki Hagiwara, Kazuhiko Minami, Yasuo Narumi, and Koichi Kindo. Physical Review B **72** (2005) 024459.
[10] M Hagiwara, Y Narumi, K Minami, and K Kindo. Physica B: Condensed Matter 294 (2001) 30–33.
[11] Jie Qiao and Bin Zhou. Chinese Physics B **24** (2015) 110306.
[12] Yi-Dan Zheng, Zhu Mao, and Bin Zhou. Chinese Physics B **26** (2017) 070302.
[13] Yidan Zheng, Zhu Mao, and Bin Zhou. Chinese Physics B **27** (2018) 090306.
[14] J Torrico, M Rojas, SM de Souza, Onofre Rojas, and NS Ananikian. EPL (Europhysics Letters), **108** (2014) 50007.
[15] Onofre Rojas, M Rojas, NS Ananikian, and SM de Souza. Physical Review A, **86** (2012) 042330.
[16] Filippo Esposito and Grzegorz Kamieniarz. Phys. Rev. B **57** (1998) 7431–7433.
[17] Kazuo Hida. Journal of the Physical Society of Japan **63** (1994) 2359–2364.
[18] H. Kikuchi, Y. Fujii, M. Chiba, S. Mitsudo, T. Idehara, T. Tonegawa, K. Okamoto, T. Sakai, T. Kuwai, and H. Ohta. Phys. Rev. Lett. **94** (2005) 227201.
[19] Sanjit Konar, Partha Sarathi Mukherjee, Ennio Zangrando, Francesc Lloret, and Nirmalendu Ray Chaudhuri. Angewandte Chemie International Edition **41** (2002) 1561–1563.
[20] V.S. Abgaryan, N.S. Ananikian, L.N. Ananikyan, and V.V. Hovhannisyan. Solid State Communications **224** (2015) 15 – 20.
[21] V.V. Hovhannisyan, N.S. Ananikian, and R. Kenna. Physica A: Statistical Mechanics and its Applications **453** (2016) 116 – 130.
[22] V V Hovhannisyan, J Streˇcka, and N S Ananikian. Journal of Physics: Condensed Matter **28** (2016) 085401.
[23] V. Ravi Chandra and Naveen Surendran. Phys. Rev. B **74** (2006) 024421.
[24] S. Ghosh, T. F. Rosenbaum, G. Aeppli, and S. N. Nature **425** (2003) 48–51.
[25] Ulrich Glaser, Helmut B¨uttner, and Holger Fehske. Phys. Rev. A **68** (2003) 032318.
[26] Marcin Wie´sniak, Vlatko Vedral, and Caslav Brukner. New Journal of Physics **7** (2005) 258–258.
[27] Olivier Kahn. Molecular magnetism. VCH, New York, 1993.
[28] Michael E. Fisher. American Journal of Physics **32** (1964) 343–346.
[29] D. O. Soares-Pinto, A. M. Souza, R. S. Sarthour, I. S. Oliveira, M. S. Reis, P. Brandˇao, J. Rocha, and A. M. dos Santos. EPL (Europhysics Letters) **87** (2009) 40008.
[30] G. Vidal and R. F. Werner. Phys. Rev. A **65** (2002) 032314.